

Glycerol Valorization as Biofuel: Thermodynamic and Kinetic Study of the Acetalization of Glycerol with Acetaldehyde

Rui P. V. Faria, Carla S. M. Pereira,* Viviana M. T. M. Silva, José M. Loureiro, and Alírio E. Rodrigues

Laboratory of Separation and Reaction Engineering (LSRE), Associate Laboratory LSRE/LCM, Faculdade de Engenharia, Universidade do Porto, Rua Dr. Roberto Frias, 4200-465 Porto, Portugal

Supporting Information

ABSTRACT: The work reported in this article is a thermodynamic and kinetic study of the acetalization reaction between acetaldehyde and glycerol to produce glycerol ethyl acetal (GEA). A catalyst screening was performed allowing for the choice of Amberlyst-15 wet resin as the most suitable catalyst for this reaction. Through the study of the reaction thermodynamic equilibrium, it was possible to determine the value of the equilibrium constant as a function of temperature, $\ln(K) = 1.419 + 1055/T$, and the corresponding thermodynamic parameters $\Delta H_{298\text{ K}}^0 = -8.77 \text{ kJ}\cdot\text{mol}^{-1}$ and $\Delta G_{298\text{ K}}^0 = -12.3 \text{ kJ}\cdot\text{mol}^{-1}$. Additionally, the standard enthalpy and Gibbs free energy of formation of GEA were also obtained, as -584.4 and $-387.0 \text{ kJ}\cdot\text{mol}^{-1}$, respectively. The Langmuir–Hinshelwood–Hougen–Watson model considering internal mass-transfer limitations presented the best fitting of the reaction kinetic behavior. The parameters estimated for this model were $k_c (\text{mol}\cdot\text{g}_{\text{cat}}^{-1}\cdot\text{s}^{-1}) = 3.13 \times 10^9 - 6223/T$ and $K_{S,W} = 1.82 \times 10^{-3} \exp(2361/T)$. The acetalization of glycerol with acetaldehyde presents an activation energy of $51.7 \text{ kJ}\cdot\text{mol}^{-1}$.

1. INTRODUCTION

In recent times, it has become clear that the world's dependence on fossil fuels for energy has a significant negative environmental impact. This fact, along with the petroleum market fluctuations due to political instability in producer countries, have prompted the development of alternatives to fossil resources and the implementation of “greener” policies.

Biodiesel, on the other hand, constitutes a renewable resource that seems to overcome the implications brought by the excessive use of fossil fuels. Compared to petroleum-derived diesel, it presents the advantages of reduced toxicity and exhaust emissions, for instance, and consequently, its production has significantly increased over the past few years.

Biodiesel is defined as a methyl ester obtained through the transesterification of vegetable oils and animal fats with methanol in the presence of an acid or basic catalyst (European Union Directive 2009/28/EC). About 10% (w/w) glycerol is obtained as the main byproduct in biodiesel production. Therefore, glycerol is becoming widely available at lower prices, because its conventional market cannot absorb this surplus, turning it into an interesting raw material for the synthesis of new value-added products.

Among possible glycerol-based products,^{1–3} acetals have drawn the attention of several research groups. In addition to classical acetal applications (protecting group or starting material in organic synthesis,⁴ fragrance and flavoring agent⁵), cyclic acetals derived from glycerol, in particular, glycerol ethyl acetal (GEA), are generally recognized as effective fuel additives. Previous studies have shown that GEA presents the ability to reduce particulate emissions of exhaust gases without having any negative impact on engine performance^{6,7} and, simultaneously, to allow for the control of fuel fluid properties, including cloud point, viscosity, and freezing point.^{8–12} In addition, these glycerol acetals are completely soluble in fatty

acid esters (FAEs) and, at almost all proportions, in diesel,^{9,13} although they present some solubility problems with gasoline.¹⁴

GEA consists of an isomeric mixture of five- and six-membered ring acetals in both *cis* and *trans* forms including the following compounds: *cis*-5-hydroxy-2-methyl-1,3-dioxane, *trans*-5-hydroxy-2-methyl-1,3-dioxane, *cis*-4-hydroxymethyl-2-methyl-1,3-dioxolane, and *trans*-4-hydroxymethyl-2-methyl-1,3-dioxolane.¹⁵ There are two main routes for the synthesis of this product: direct acetalization of glycerol with acetaldehyde^{15–20} (eq 1) and transacetalization by reacting glycerol with 1,1-diethoxyethane (DEE).^{6,21–23} The acetalization route was used in this work, because its only disadvantage is the formation of water, which is undesirable in the final fuel additive. However, water-free GEA solution can be obtained by the use of an integrated reaction–separation technology, such as the simulated moving-bed reactor, which has already proved to be efficient in other acetalization processes.^{24–27} Moreover, this route avoids the more complex reaction scheme of the transacetalization process with several reaction and separation units (usually, one reactor for the production of DEE from acetaldehyde and ethanol, a distillation column for separating DEE, a reactor for the synthesis of GEA from DEE and glycerol, and a distillation column for separating the final product¹⁶). It presents a better reaction mass efficiency²⁸ and depends only on a feedstock that can be obtained from biomass: Glycerol is a byproduct from biodiesel production, as previously mentioned, and acetaldehyde is produced from bioethanol.²¹

Received: October 26, 2012

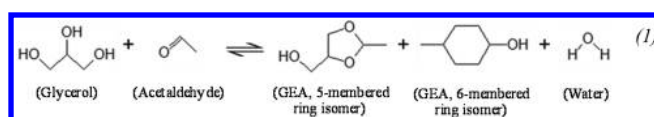
Revised: January 7, 2013

Accepted: January 9, 2013

Published: January 9, 2013

Table 1. Properties of the Ion-Exchange Resins

ion-exchange resin	type	physical form	particle size (mm)	ion-exchange capacity (equiv·kg ⁻¹)	surface area (m ² ·g ⁻¹)
Amberlyst-15 (wet)	strong acid	opaque beads	0.600–0.850	4.7	53
Amberlyst-35 (wet)	strong acid	opaque beads	0.700–0.950	5.2	50
Amberlyst-36 (wet)	strong acid	opaque beads	0.600–0.850	5.4	33
Amberlyst-46 (wet)	strong acid	opaque beads	NA	0.43	75
Amberlyst-47 (wet)	strong acid	opaque beads	NA	NA	NA
Amberlyst-70 (wet)	strong acid	opaque beads	0.500	2.65	36
Amberlyst-CH28 (wet)	strong acid	opaque beads	0.850–1.050	4.8	36
Nafion SAC-13	strong acid	granules	8–50 (mesh)	0.12–1.00	200



The mechanism proposed for this reaction¹⁵ comprises the formation of an hemiacetal from a glycerol primary or secondary hydroxyl group (considered the limiting step) and its dehydration, forming a carbocation that, through a nucleophilic substitution mechanism (S₂N) with an oxygen from one of the remaining hydroxyl groups of the glycerol molecule, leads to the closure of the heteroatom ring, thereby forming the cyclic acetal. Depending on which hydroxyl group (primary or secondary) is involved in each step, the product of the reaction might be the six- or five-membered ring isomer.

Few studies about the synthesis of GEA have been published to date, and most of them present some inconsistencies^{16,17} or make use of solvents and/or homogeneous catalysts.^{15,19} However, a heterogeneous catalyzed continuous process for the synthesis of GEA was reported by Miller et al.²¹ In this process, GEA is produced by reacting the outlet stream of a transesterification reactor, containing an FAE and glycerol, with acetaldehyde. A mixture comprising the fuel and the GEA additive is obtained as the outlet stream without the need to introduce the additive in the fuel composition at another stage of the process. However, the assessment of this process was conducted only by computational simulation using Aspen Plus software. The major drawbacks of this process are related to the complex reaction scheme and the formation of water during the synthesis of GEA, which can lead to the hydrolysis of the FAE and promote the decrease of the catalytic activity of the ion-exchange resin. Nevertheless, its benefits are clear, because it not only suggests a continuous process for the production of a biodiesel containing a glycerol acetal additive that reduces biodiesel particulate emissions, but is also able to increase the process yield by approximately 13% through the incorporation of glycerol (in GEA form) in the final product, eliminating the high costs and energy requirements for the separation of this alcohol.

In earlier works,^{23,29} the synthesis and separation of GEA isomers were achieved by means of a batch reaction followed by a simple distillation or a reactive distillation (either batch or continuous) with the purpose of producing the pure GEA six-membered ring isomer to be used in the synthesis of 1,3-dihydroxyacetone. The reaction between glycerol and DEE, in a molar ratio of 1:1, was carried in the presence Amberlyst-15 (1.7 wt %) at 318.2 K. After 4 h of reaction, the heterogeneous catalyst was separated by filtration, and the unreacted DEE and ethanol (byproduct) were eliminated by vacuum distillation ($P = 0.03$ bar, $T = 343.2$ K). The use of a simple batch distillation process led to a final product containing over 90 wt % of the desired isomer; however, it was possible to recover only 55% of

its initial amount. By a batch reactive distillation, using Amberlyst-15 as the catalyst for isomer interconversion, it was also possible to obtain a highly concentrated product (>90 wt %), and the recovery was increased to 66%. The authors also demonstrated that the continuous production of the intended isomer by the reactive distillation of the isomeric mixture is possible, obtaining an outlet stream of the final product with specifications similar to those obtained through the batch process.

Acetalizations are equilibrium-limited acid-catalyzed exothermic reactions. Several catalysts, such as inorganic acids (chloridric acid,³⁰ *p*-toluene sulfonic acid³¹), ion-exchange resins (Amberlyst-15,³² Amberlyst-36³³), zeolites (HSZ 36,³⁴ ZSM5³¹), silica-based mesoporous materials (MoO₃/SiO₂,³⁵ MCM-41³⁶), Lewis acids (AuCl₃³⁰), ionic liquids ([Hmim]₃PW₁₂O₄₀³⁷), and clay minerals (Montmorillonite K-10³³) have been suggested for acetalization reactions over a wide range of operating conditions. The benefits of heterogeneous catalysis over homogeneous catalysis are well-known and are mainly related with the ease of separation and purification of the desired product and the absence of the need for neutralization steps. Among the heterogeneous catalysts mentioned, aluminosilicates, such as zeolites, present good performances; however, acid ion-exchange resins have been demonstrated to be particularly effective for this type of reaction, achieving higher yields (approximately 80%) in short periods of time.^{33,38}

In the current work, an extensive study of the acetalization of glycerol with acetaldehyde was conducted, aiming at the valorization of glycerol through its conversion into compounds useful as fuel additives. Thus, relevant data were collected to determine the dependence of the chemical equilibrium constant on temperature and to estimate the reaction standard Gibbs free energy, ΔG^0 , and standard enthalpy, ΔH^0 , considering a nonideal liquid-phase model determining the activity of each species through the UNIFAC group contribution method. The study of the reaction kinetics started with a screening of catalysts, with particular focus on acid ion-exchange resins and zeolites. Once the most suitable catalyst had been selected, the effects of several variables on the reaction rate were experimentally evaluated with the purpose of finding a model that gives an accurate description of the reaction kinetics over a wide range of operating conditions. Two reaction rate laws were assessed: the pseudohomogeneous and Langmuir–Hinshelwood–Hougen–Watson models. The influence of the diffusion of the species inside the catalyst particles was considered.

2. EXPERIMENTAL DESCRIPTION

2.1. Chemicals and Catalysts.

The chemicals used were 2-propanol (>99.9%), 1-butanol (>99.9%), acetaldehyde (>99%),

and glycerol (>99% in water) from Sigma-Aldrich (Dorset, U.K.).

Several commercial strong-acid ion-exchange resins (Rohm & Haas) were tested as catalysts. Table 1 presents their brief characterization.

To avoid any decrease of the reaction rate, because water (one of the reaction products) adsorbs on the surface of the catalyst, it was necessary to guarantee anhydrous resin. For this reason, prior to use, the resin was washed several times with deionized water, then washed with ethanol, and finally dried at 363.15 K until the mass remained constant.

Zeolites H-BEA 25, H-MFI 90, H-MOR 20 and Molecular Sieve 3A supplied by Süd-Chemie were also tested as catalysts with and without previous conditioning. The conditioning consisted of several washes with ethanol followed by 3 h of calcination at 773.15 K.

2.2. Experimental Setup and Procedure. **2.2.1. Catalyst Screening.** Reactions were carried out in a glass 100 mL closed vessel operating in batch mode at atmospheric pressure. Samples were collected with a syringe through a sampling tube immersed in the reaction medium. The mixture was stirred and kept at 293.15 K with a thermostatic water bath. Equimolar mixtures of glycerol and acetaldehyde (~48 mL) were prepared, and the reactions were carried out in the presence of a catalyst weight percentage of 1% relative to the total mass at 1 bar. For these conditions, vapor–liquid equilibrium (VLE) calculations showed that the total number of moles in the vapor phase represented 0.3% of the number of moles in the liquid phase, and 50% of the number of moles in the gas phase above the liquid was acetaldehyde.

The catalysts that presented the best performances in the initial experiments were further tested on a glass-jacketed 1 L closed vessel (Büchi Laboratory Equipment, Flawil, Switzerland), operating in batch mode, equipped with pressure and temperature sensors and a blow-off valve (Figure 1) and mechanically stirred at 450 rpm. The temperature was kept at 323.15 K through a water bath (LAUDA, Lauda-Königshofen, Germany). The pressure was set to 8.0 bar to keep the reaction mixture in the liquid phase.

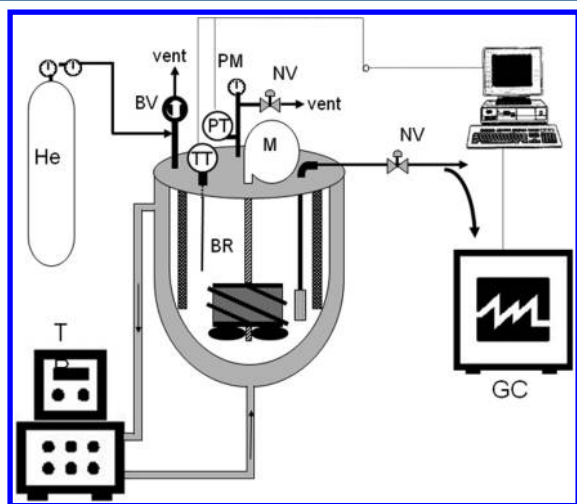


Figure 1. Scheme of the experimental setup used for kinetic experiments. BR, batch reactor; M, motor; TT, temperature sensor; PT, pressure sensor; PM, manometer; NV, needle valve; GC, gas chromatograph; T, thermostatic bath.

2.2.2. Thermodynamic Equilibrium Experiments. Thermodynamic equilibrium experiments were carried out in a 150 mL stainless steel batch reactor equipped with temperature and pressure sensors. Heat was provided through a heating plate with external temperature control of the reaction media. A connection to a helium pressurized line allowed pressure control.

Experiments were performed at temperatures within the range of 298.15–362.23 K. To keep the reaction mixture in the liquid phase over the whole operating temperature range, the pressure was set to 8.0 bar with helium. Different initial compositions were tested. The reactions proceeded until no further changes in the composition were detected.

2.2.3. Kinetic Experiments. The kinetic studies were carried out in the reaction setup presented in Figure 1.

The effects of parameters such as stirring speed (250–450 rpm), catalyst average particle diameter (512.5 and 720 μm) and loading (0.2 and 0.4 wt % of the total mass of the reaction medium), temperature (313.15–358.15 K), and initial composition were evaluated. The pressure was set to 8.0 bar with helium, to keep all of the compounds in the liquid phase. The vapor pressures of acetaldehyde and glycerol are 6.65 bar and approximately zero, respectively, at 90 °C, which was the highest temperature studied. At 8 bar, for an equimolar mixture of acetaldehyde and glycerol (~760 mL), VLE calculations showed that the total number of moles in the vapor phase was 0.5% of the total number of moles in the liquid phase and that 56% of the gas was helium.

2.2.4. Analytical Methods. All samples were analyzed in a gas chromatograph (Shimadzu, GC 2010 Plus) using 2-propanol as the solvent and 1-butanol as the internal standard. The compounds were separated using a silica capillary column (CPWax52CB, 25 m \times 0.25 mm i.d., film thickness of 1.2 μm) and quantified by a thermal conductivity detector. Helium N50 was used as the carrier gas at a flow rate of 9.4 mL \cdot min $^{-1}$. The temperatures of the injector and thermal conductivity detector were set to 573.15 K. The initial column temperature was 383.15 K for 2.2 min; the temperature was then increased at 10 K \cdot min $^{-1}$ to 513.15 K and subsequently held constant for the following 7 min.

3. RESULTS AND DISCUSSION

3.1. Catalyst Screening. Considering the open literature,^{30–37} a screening of several commercial acid catalysts was performed, with particular focus on Amberlyst and Nafion acid ion-exchange resins (Table 1) and zeolites H-BEA 25, H-MFI 90, H-MOR 20, and Molecular Sieve 3A, to find the most suitable catalyst for GEA synthesis (Figure 2).

From Figure 2, it is possible to conclude that, over an 8-h period at the mentioned operating conditions, Amberlyst-15 was the most active catalyst for this reaction, leading to conversions slightly higher than 80%. A conversion of approximately 78% was achieved for Amberlyst-35, Amberlyst-36, and Amberlyst-47, whereas for Amberlyst-46, Amberlyst-70, and Amberlyst-CH28, the value was near 75%. With a conversion of approximately 40%, Nafion SAC-13 was the ion-exchange resin that presented the lowest activity.

Zeolites, on the other hand, presented significantly lower conversion values. Experiments showed that the conditioning of the zeolites before their use had a significant influence on their activity. An increase in the conversion from 8% to 20% was observed, for instance, between the zeolite H-BEA 25 samples that were not subjected to previous conditioning compared to

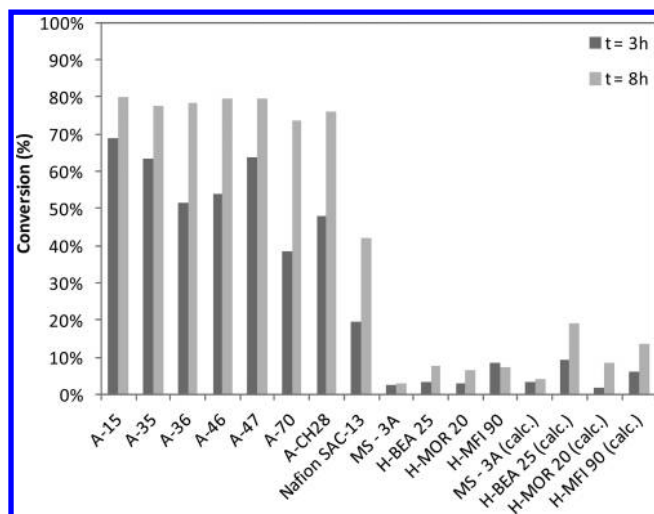


Figure 2. Catalyst performances in terms of glycerol conversion after 3 and 8 h ($T = 293.15$ K, $P = 1.0$ bar, initial acetaldehyde/glycerol molar ratio = 1:1, $w_{\text{cat}} = 1$ wt %).

those that were. However, the activities of the zeolites were still insufficient, and therefore, the zeolites were considered as unsuitable catalysts for this acetalization reaction. This unexpectedly low activity of zeolites comparing with what is reported in the literature^{31,34} might be related to either the low temperature at which the experiments were performed or a possible hindrance caused by the adsorption of water (formed as a byproduct of this reaction) because zeolites are well-known for their dehydrating capacity.

Although Amberlyst-15 was found to have the highest catalytic activity throughout the entire experiment, the performances of Amberlyst-35 and Amberlyst-47 were noticeably high, and for that reason, all three of these ion-exchange resins were considered as possible catalysts for this reaction and were thus subjected to further tests at 323.15 K (with all other variables kept the same). The results of these tests are shown in Figure S1 (Supporting Information) and demonstrate that, even for higher temperatures, Amberlyst-15 presented the best kinetic results, even though Amberlyst-35 presents a higher acidity (Table 1). This result should be caused by the higher surface area and smaller particle diameter of Amberlyst-15 (when compared with Amberlyst-35), which leads to higher accessibility to the acid sites of the catalyst and lower diffusion rates inside the pores of the pellet to reach the internal active acid sites, respectively. Consequently, Amberlyst-15 was selected as the most suitable catalyst for the production of GEA using chromatographic reactors, such as the simulated moving-bed reactor, operated at moderate temperatures.

3.2. Thermodynamic Equilibrium. Considering the nonideal liquid-phase reaction between acetaldehyde and glycerol (eq 1), the chemical equilibrium constant, K , can be expressed as

$$K = \prod_i a_i^{\nu_i} = \frac{a_{\text{GEA}} a_{\text{W}}}{a_{\text{Ac}} a_{\text{Gly}}} = \frac{x_{\text{GEA}} x_{\text{W}} \gamma_{\text{GEA}} \gamma_{\text{W}}}{x_{\text{Ac}} x_{\text{Gly}} \gamma_{\text{Ac}} \gamma_{\text{Gly}}} \quad (2)$$

where a_i is the activity of compound i , ν_i is the stoichiometric coefficient of compound i in the reaction, x_i is the molar fraction of compound i , and γ_i is the activity coefficient of compound i .

For the computation of the activity coefficients, the universal functional activity coefficient (UNIFAC) model was applied.

This group contribution method requires the use of parameters such as the relative molecular volumes and surface areas of pure species, as well as the interaction parameters between the different groups of each molecule. The values for these parameters are presented in the Supporting Information (Tables S1 and S2).

It should be noticed that, for the application of the UNIFAC model to this system, the same group partition was assumed for all GEA isomers, allowing the handling of the isomeric mixture as a single compound.

A summary of the initial conditions and the results obtained in the experiments performed for the assessment of the thermodynamic chemical equilibrium is presented in Table S3 (Supporting Information).

Through its most general definition, the chemical equilibrium constant can be expressed as a function of the reaction standard Gibbs free energy, ΔG^0 , and temperature, T , according to the equation

$$K = \exp\left(-\frac{\Delta G^0}{RT}\right) = \prod_i a_i^{\nu_i} \quad (3)$$

where R is the ideal gas constant. Furthermore

$$\Delta G^0 = \Delta H^0 - T\Delta S^0 \quad (4)$$

where ΔH^0 and ΔS^0 are the reaction standard enthalpy and entropy, respectively. Thus, combining eqs 3 and 4 and plotting $\ln(K)$ versus $1/T$ (Figure 3), it is possible to determine the

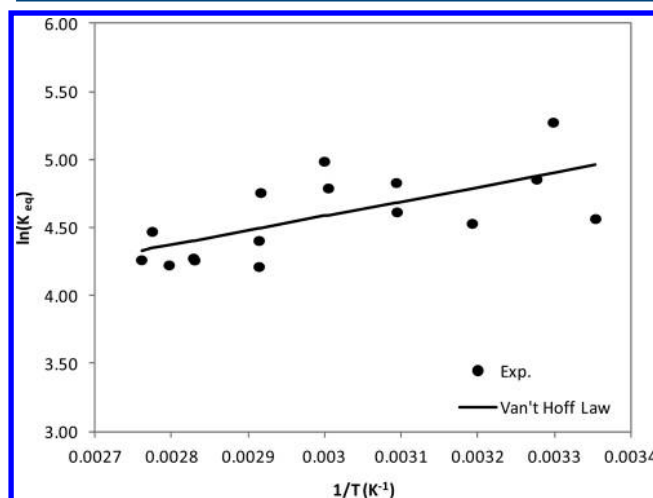


Figure 3. Linearization of the values of equilibrium constants according to the van't Hoff equation.

dependence of the equilibrium constant on temperature, which can be expressed as $\ln(K) = 1.419 \pm 0.96 + (1055 \pm 320)/T$, so that the values for the two thermodynamic parameters are $\Delta H_{298\text{ K}}^0 = -8.77 \pm 2.7$ kJ·mol⁻¹ and $\Delta G_{298\text{ K}}^0 = -12.3 \pm 2.4$ kJ·mol⁻¹. Because the enthalpy value is negative, one can conclude that this is an exothermic reaction.

A standard property change for a reaction, ΔM^0 , can be determined as

$$\Delta M^0 = \sum_i \nu_i \Delta M_i^0 \quad (5)$$

Considering the parameters determined for the acetalization reaction under study and the values for the standard enthalpy and Gibbs free energy of formation of acetaldehyde, glycerol,

and water found in the literature (DIPPR Database³⁹), it is possible to obtain an estimate of these standard properties for GEA, as follows: $\Delta H_{f,GEA}^0 = -584.4 \text{ kJ}\cdot\text{mol}^{-1}$ and $\Delta G_{f,GEA}^0 = -387.0 \text{ kJ}\cdot\text{mol}^{-1}$. These values are listed in Table 2. To the best of our knowledge, this is the first time that these data have been presented in the open literature.

Table 2. Standard Enthalpies and Gibbs Free Energies of Formation for All Species

compound	$\Delta H_{f,i}^0$ (kJ·mol ⁻¹)	$\Delta G_{f,i}^0$ (kJ·mol ⁻¹)
acetaldehyde ³⁹	-166.4	-133.3
glycerol ³⁹	-669.6	-478.6
water ³⁹	-285.8	-273.2
GEA ^a	-584.4	-387.0

^aThis work.

3.3. Reaction Kinetic Studies. This section presents the experimental results and modeling for the kinetics of the acetalization reaction for the production of GEA (eq 1) using Amberlyst-15 as catalyst.

A mathematical model was implemented considering a batch reactor operating under isothermal conditions. The existence of external mass-transfer limitations was assessed by performing experiments at different stirring speeds (see Figure S2 of the Supporting Information). The results showed that, when the stirring speed was set to 450 rpm, the mass-transfer resistance was negligible. Therefore, all subsequent experiments were performed at a stirring speed of 450 rpm. On the other hand, the possibility of the existence of internal mass-transfer limitations of the species through the catalyst particles pores was considered. Amberlyst-15 has a bidisperse pore size distribution containing micro- and macropores.^{40,41} The reactants should first diffuse through the macropores to the external surface of microspheres and then penetrate into the gel phase. In this work, diffusion through the macropores of the particles and reaction at the microsphere active sites were considered. Diffusion inside the gel microspheres was considered to be infinitely fast. This approach has been corroborated by several works.^{40,42–44}

Thus, the mass balances for the bulk and intraparticle fluid can be written as

$$\frac{dC_{b,i}}{dt} = -\frac{3}{R_p} \left(\frac{1 - \varepsilon_b}{\varepsilon_b} \right) D_{\text{eff},i} \left. \frac{\partial C_{p,i}}{\partial r} \right|_{r=R_p} \quad (6)$$

$$\varepsilon_p \frac{dC_{p,i}}{dt} = \frac{1}{r^2} \frac{\partial}{\partial r} \left(D_{\text{eff},i} r^2 \frac{\partial C_{p,i}}{\partial r} \right) + (1 - \varepsilon_p) \nu_i \rho_p R \quad (7)$$

respectively, where the index i refers to a reaction species (acetaldehyde, glycerol, GEA, or water); $C_{b,i}$ and $C_{p,i}$ represent the molar concentrations evaluated in the bulk and intraparticle fluid, respectively; R_p represents the catalyst particle radius; $D_{\text{eff},i}$ is the effective diffusion coefficient; ε_b and ε_p are the bulk and the catalyst particle porosities, respectively; ρ_p is to the catalyst density; ν_i is the stoichiometric coefficient; and R is the reaction rate based on the local intraparticle composition. The method for computing the effective diffusion coefficients can be found in the Supporting Information. For that purpose, the dependence of the viscosity and density on temperature for glycerol, acetaldehyde, and water was obtained from the literature,⁴⁵ whereas for GEA, these physical properties had

to be determined experimentally (Supporting Information) because such data were not available. For the range of temperatures studied, the following relations were obtained for the GEA viscosity (μ) and density (ρ)

$$\log[\mu \text{ (cP)}] = \frac{1255}{T} - 4.286 \quad (8)$$

$$\rho \text{ (g}\cdot\text{cm}^{-3}) = -7.723 \times 10^{-4} T + 1.355 \quad (9)$$

For this model, one can assume the following initial conditions

$$t = 0 \rightarrow C_{b,i} = C_{b,i,0} \quad (10)$$

$$t = 0 \rightarrow C_{p,i} = C_{p,i,0} \quad (11)$$

and boundary conditions

$$r = 0 \rightarrow \frac{\partial C_{p,i}}{\partial r} = 0 \quad (12)$$

$$r = R_p \rightarrow C_{b,i} = C_{p,i}|_{r=R_p} \quad (13)$$

The reaction rate was described by two different models: pseudohomogeneous (PH) and Langmuir–Hinshelwood–Hougen–Watson (LHHW). The PH model considers a reversible reaction of first order in each species and can be expressed in terms of activities as

$$R = k_c \left(a_{\text{Ac}} a_{\text{Gly}} - \frac{a_{\text{GEA}} a_{\text{W}}}{K} \right) \quad (14)$$

where k_c represents the reaction kinetic constant.

The LHHW model has already been used to describe the reaction of acetaldehyde with several linear chain alcohols (methanol,⁴⁶ ethanol,^{44,47} and butanol⁴⁸). As stated by previous authors, this model comprises the adsorption of both reactants, the surface reaction between them to form an adsorbed hemiacetal, surface reaction with the formation of water (considered the rate-determining step), surface reaction with the formation of the acetal, and desorption of both products. Additionally, water has been demonstrated to adsorb more than all other species. Therefore, the LHHW model can be expressed by the simplified expression

$$R = k_c \frac{\left(a_{\text{Ac}} a_{\text{Gly}} - \frac{a_{\text{GEA}} a_{\text{W}}}{K} \right)}{1 + K_{\text{S,W}} a_{\text{W}}} \quad (15)$$

where $K_{\text{S,W}}$ represents the water adsorption equilibrium constant.

The temperature dependence of the reaction kinetic and equilibrium adsorption constants is expressed by the Arrhenius (eq 16) and van't Hoff (eq 17) equations, respectively

$$k_c = k_{c,0} \exp\left(-\frac{E_a}{RT}\right) \quad (16)$$

$$K_{\text{S,W}} = K_{\text{S,W}0} \exp\left(-\frac{\Delta H_{\text{S,W}}}{RT}\right) \quad (17)$$

The commercial software gPROMS (General Process Modeling System, version 3.4.0) was used to solve the model equations (eqs 6–17) and to estimate the values of the unknown parameters (E_a and $k_{c,0}$ for the PH model and E_a , $k_{c,0}$, $\Delta H_{\text{S,W}}$, and $K_{\text{S,W}0}$ for the LHHW model). The partial differential equations were treated using gPROMS numerical

solver, DASOLV (based on the method of lines), discretizing the radial domain through a centered finite-element method of second order and using 28 (nonuniform) discretization intervals. The estimation of the parameters for the proposed reaction rate models was carried out using the gPROMS "Parameter Estimation" tool. The experimental data were fitted by the maximum likelihood method. Its objective function is given by

$$\Phi = \frac{N}{2} \ln(2\pi) + \frac{1}{2} \min_{\theta} \left\{ \sum_{j=1}^{NE} \sum_{k=1}^{NM_j} \left[\ln(\sigma_{jk}^2) + \frac{(X_{jk}^{\text{exp}} - X_{jk}^{\text{mod}})^2}{\sigma_{jk}^2} \right] \right\} \quad (18)$$

where θ is the set of parameters to be estimated; X_{jk}^{exp} and X_{jk}^{mod} are the k th measured and predicted values, respectively, for the conversion in experiment j ; σ_{jk}^2 is the variance in conversion; N represents the total number of measurements during all experiments; NE represents the number of experiments performed; and NM_j represents the number of measurements of conversion values made in experiment j . The parameter estimation tolerance was set to 10^{-5} , and a constant-variance model was assumed.

To determine the unknown constants of the model, a parametric study was performed in which the effects of changes in design variables such as the initial reaction medium composition, temperature, catalyst loading, and particle size were assessed, according to the experiments presented in Table 3.

Table 3. Operating Conditions Used in Kinetic Experiments

no.	temperature (K)	initial molar ratio	catalyst loading (wt _{cat} wt %)	pressure (bar)	catalyst particle size (μm)
1	358.0	1.00	0.4	8.0	685.0
2	353.2	1.00	0.4	8.0	685.0
3	333.2	1.00	0.4	8.0	685.0
4	313.2	1.00	0.2	8.0	685.0
5	333.2	1.00	0.2	8.0	685.0
6	353.2	1.00	0.2	8.0	685.0
7	313.2	1.25	0.2	8.0	685.0
8	353.2	1.00	0.13	8.0	512.5
9	353.2	1.00	0.13	8.0	720.0
10	322.9	1.00 ^a	0.2	8.0	685.0
11	342.9	1.00 ^b	0.2	8.0	685.0

^aInitial reaction mixture contained 7.0% water and 7.0% GEA. ^bInitial reaction mixture contained 15.0% water and 15.0% GEA.

From experiments 1–6, a first estimate for an apparent reaction activation energy ($E_a = 26.1 \text{ kJ}\cdot\text{mol}^{-1}$) was obtained by the initial-reaction-rate method and the Arrhenius equation.

Table 4. Estimated Kinetic Parameters for the PH and LHHW Models and Respective Objective Function Values

	PH	PH with mass-transfer resistance	LHHW	LHHW with mass-transfer resistance
E_a (kJ·mol ⁻¹)	38.8	60.4	38.7	51.7
k_{c0} (mol·g _{cat} ⁻¹ ·min ⁻¹)	1.14×10^6	2.79×10^{10}	1.14×10^6	3.13×10^9
$\Delta H_{S,W}$ (kJ·mol ⁻¹)	–	–	–24.8	–19.6
$K_{S,W0}$	–	–	2.05×10^{-6}	1.82×10^{-3}
F_{obj}/NE	–29.7	–26.9	–29.5	–31.1

This value was used as an initial estimate for the activation energy of the parameter estimations. When adsorption was included in the reaction rate law, the value determined by Graça et al.⁴⁸ for the water enthalpy of adsorption ($\Delta H_{S,W} = -27.5 \text{ kJ}\cdot\text{mol}^{-1}$) was used as the initial estimate for this variable. Table 4 summarizes the results obtained by the parameter estimation procedure implemented for both the PH and LHHW reaction rate laws considering both the absence and presence of internal mass-transfer resistances.

The increase observed in the value of the activation energy when resistance to the diffusion of the compounds through the catalyst particles pores was considered (for both the PH and LHHW models) is an indication that this phenomenon must be taken into account (as evidenced by the experimental results shown in Figure 9, below). Considering this fact and the results presented in Table 4, one can conclude that the LHHW model including intraparticle mass-transfer limitations can describe the experimental results more accurately than the other models tested, as it presents the lowest value for the objective function. For this model, it was possible to determine a reaction activation energy of $51.7 \text{ kJ}\cdot\text{mol}^{-1}$ and a water enthalpy of adsorption of $-19.6 \text{ kJ}\cdot\text{mol}^{-1}$.

A more detailed discussion of the behavior of the selected kinetic model is performed in the following sections by comparison with the experimental results obtained from the parametric studies that were performed.

3.3.1. Effect of Catalyst Loading. The increase of the catalyst loading, from 0.2 to 0.4 wt % (mass of catalyst over the total mass of reactants), was experimentally tested (Figure 4)

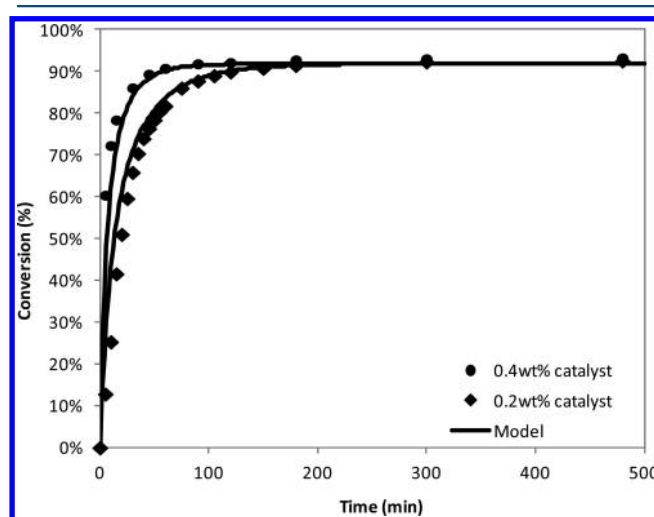


Figure 4. Effect of the catalyst amount on the reaction rate ($T = 313.2 \text{ K}$, $P = 8.0 \text{ bar}$, initial acetaldehyde/glycerol molar ratio = 1:1, unsieved Amberlyst-15, stirring speed = 450 rpm).

and led to an expected increase in the initial reaction rate of approximately 50%. This fact is due to the increase in the

number of acid catalytic sites. The model correctly describes the effect of the increase and decrease of catalyst loading.

3.3.2. Effect of Temperature. Experiments were performed at temperatures ranging from 313.2 to 358.0 K to assess the effect of this variable on the reaction rate. Once again, the experimental results and the model presented the same behavior. The conversion versus time plot presented in Figure 5 shows that, as the temperature increased, the reaction became

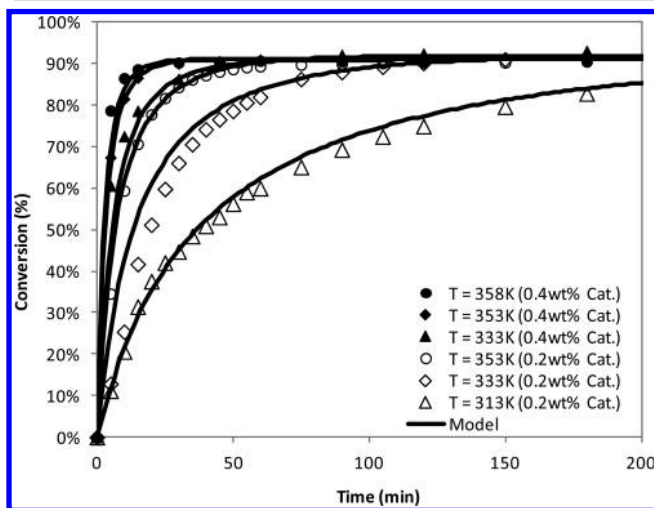


Figure 5. Effect of temperature on the reaction rate ($P = 8.0$ bar, initial acetaldehyde/glycerol molar ratio = 1:1, unsieved Amberlyst-15, stirring speed = 450 rpm).

faster. However, the equilibrium conversion decreased for higher temperature values as a consequence of the exothermic character of the acetalization of glycerol.

3.3.3. Effect of Initial Composition of the Reaction Medium. The conversion as a function of time for an equimolar mixture of glycerol and acetaldehyde was compared with the conversion for a mixture with an acetaldehyde/glycerol molar ratio of 1.25 to analyze the effect of the initial molar ratio of the reactants. From the results shown in Figure 6, it can be observed that the reaction proceeded faster when one of the

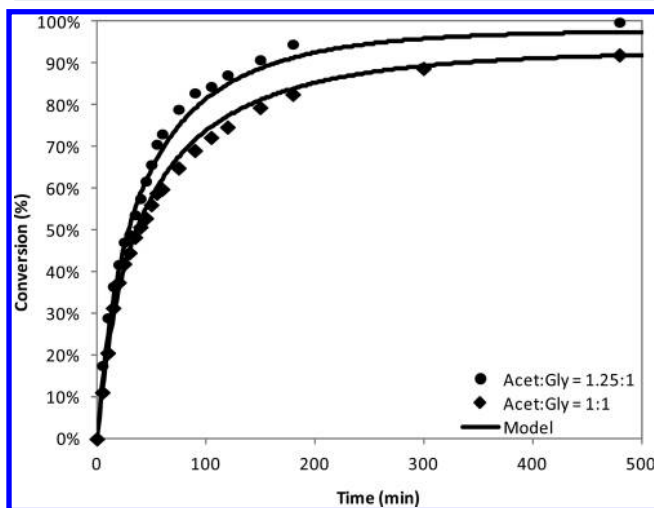


Figure 6. Effect of the initial reactant molar ratio on the reaction rate ($T = 313.2$ K, $P = 8.0$ bar, $w_{\text{cat}} = 0.2$ wt %, unsieved Amberlyst-15, stirring speed = 450 rpm).

reactants was used in excess, as could be predicted by the implemented model. The effect of the presence of the products in the initial reaction mixture was also tested (Figure 7). As

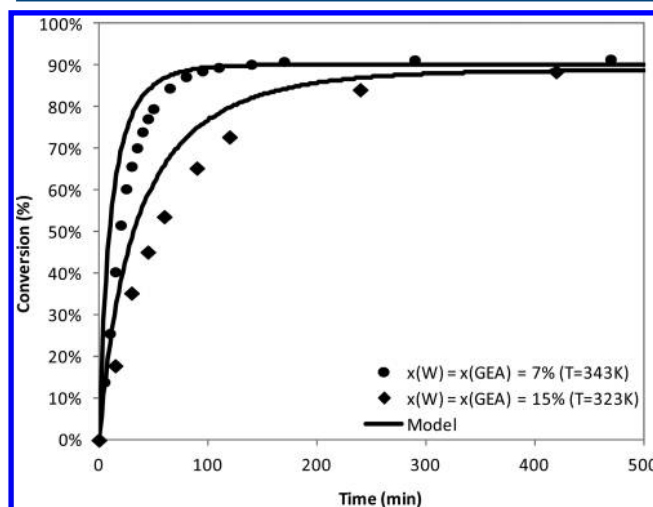


Figure 7. Effect on the reaction rate of the presence of products in the initial mixture. (●) $T = 342.9$ K, $P = 8.0$ bar, $w_{\text{cat}} = 0.2$ wt %, unsieved Amberlyst-15, stirring speed = 450 rpm; (◆) $T = 322.9$ K, $P = 8.0$ bar, $w_{\text{cat}} = 0.2$ wt %, unsieved Amberlyst-15, stirring speed = 450 rpm.

expected, the initial reaction rate was lower when GEA and water were introduced into the initial mixture. These results are related to the change in the “driving force” to reach equilibrium promoted by the different initial compositions of the reaction medium. The model does not fit this behavior as accurately as for the other experiments. The reaction rate predicted by the model was slightly higher than the experimental value. However, the results are still satisfactory.

3.3.4. Evaluation of Internal Mass-Transfer Limitations. The evaluation of internal resistances to mass transfer was based on the change in the reaction rate as a consequence of the use of catalyst particles with different sizes (because the concentration of acid sites present in Amberlyst-15 was confirmed to be independent of the particle size⁴⁹). The kinetic behaviors of particles with average diameters of 512.5 and 720 μm were compared. The difference between the conversion curves presented in Figure 8 indicates that there are some resistances to mass transfer under the tested operating conditions; however, the influence of this phenomenon could be properly predicted by the LHHW model with diffusion.

Because Amberlyst-15 is commercialized with an average particle diameter of approximately 685 μm , this phenomenon must be taken into account when this resin is used without any control of the particle diameter. Figure 9 shows the simulated internal concentration profiles for average catalyst particle diameters of 512.5 μm , 685 μm (commercial Amberlyst-15), and 720 μm at a temperature of 358.0 K, the highest temperature in the range studied, at which the higher diffusion limitation occurs.

The concentration profiles observed as a function of catalyst particle radius, from its surface to its center, provide more evidence supporting the conclusion that the reaction occurs under a diffusion-controlled rate. One can also conclude from Figure 9 that, as expected, this limitation becomes more significant with increasing catalyst particle diameter.

To quantify the effect of the diffusion mechanism on the reaction rate, the effectiveness factor⁵⁰ was computed for the

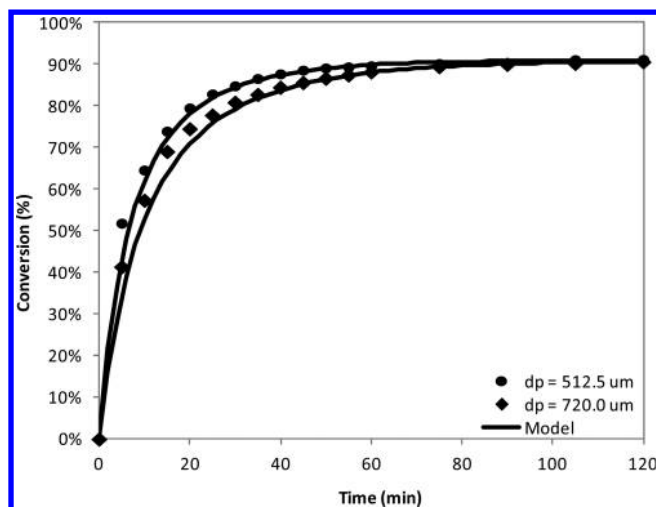


Figure 8. Effect of catalyst particle size on the reaction rate ($T = 353.2$ K, $P = 8.0$ bar, initial acetaldehyde/glycerol molar ratio = 1:1, $w_{\text{cat}} = 0.2$ wt %, stirring speed = 450 rpm).

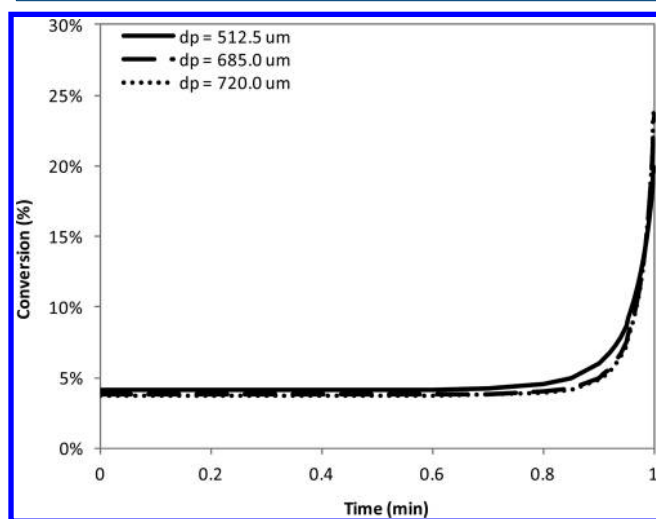


Figure 9. Effect of particle size on the glycerol concentration profile inside the catalyst, 5 min after the beginning of the reaction ($T = 358.0$ K, $P = 8.0$ bar, initial acetaldehyde/glycerol molar ratio = 1:1, $w_{\text{cat}} = 0.2$ wt %, stirring speed = 450 rpm).

previously mentioned particle diameters. The values obtained were 17%, 13%, and 12%, from the smaller to the larger particles. To be working in a complete chemically controlled regime (effectiveness factor of approximately 100%) at this temperature, an average catalyst particle diameter of less than $25 \mu\text{m}$ would be required, which is neither commercially available nor attainable from commercial resin.⁵¹

4. CONCLUSIONS

The work presented herein reports a detailed study of the condensation of glycerol with acetaldehyde, for the synthesis of GEA, from the selection of the most suitable catalyst for this reaction to the description of its thermodynamic chemical equilibrium and kinetics.

The screening of commercial catalysts performed demonstrated that acid ion-exchange resins present higher activities than zeolites. Among the tested catalysts, the best kinetic performance was achieved using Amberlyst-15.

Chemical equilibrium data were gathered for temperatures ranging from 298.15 to 362.23 K. The standard molar enthalpy and the standard Gibbs free energy values for this reaction were determined to be $\Delta H_{298\text{K}}^0 = -8.77 \text{ kJ}\cdot\text{mol}^{-1}$ and $\Delta G_{298\text{K}}^0 = -12.3 \text{ kJ}\cdot\text{mol}^{-1}$, respectively, using the UNIFAC model to determine the activities of each species. Furthermore, estimates for the standard enthalpy and Gibbs free energy of formation for GEA were also obtained, with $\Delta H_{f,\text{GEA}}^0 = -584.4 \text{ kJ}\cdot\text{mol}^{-1}$ and $\Delta G_{f,\text{GEA}}^0 = -387.0 \text{ kJ}\cdot\text{mol}^{-1}$. The experimental results showed that the reaction kinetic behavior could be accurately described by the LHHW reaction rate law, considering the existence of resistances to mass transfer inside the catalyst particles. This model considers that the surface reaction between the adsorbed reactants to produce water is the rate-determining step and that water is the preferentially adsorbed species on the surface of the ion-exchange resin catalyst.

The parametric study performed allowed for the determination of the kinetic and adsorption parameters contemplated by this model. A value of $51.7 \text{ kJ}\cdot\text{mol}^{-1}$ was determined for the reaction activation energy and a value of $-19.6 \text{ kJ}\cdot\text{mol}^{-1}$ for the water equilibrium adsorption constant.

■ ASSOCIATED CONTENT

📄 Supporting Information

Four tables and two figures. This material is available free of charge via the Internet at <http://pubs.acs.org>.

■ AUTHOR INFORMATION

Corresponding Author

*Tel.: +351 22 508 1686. Fax: +351 22 508 1674. E-mail: cpereir@fe.up.pt.

Notes

The authors declare no competing financial interest.

■ ACKNOWLEDGMENTS

The research leading to these results received funding from the European Union Seventh Framework Programme (FP7/2007-2013) under Grant Agreement 241718 EuroBioRef. This work was also financially supported by Fundação para a Ciência e a Tecnologia, Project Grant PTDC/EQU-EQU/100564/2008. C.P. gratefully acknowledges financial support from Fundação para a Ciência e a Tecnologia, Postdoctoral Research Fellowship SFRH/BPD/71358/2010.

■ NOTATION

- a_i = liquid-phase activity of compound i
- $C_{b,i}$ = molar concentration of compound i in the bulk ($\text{mol}\cdot\text{dm}^{-3}$)
- $C_{p,i}$ = molar concentration of compound i in the intraparticle fluid ($\text{mol}\cdot\text{dm}^{-3}$)
- $D_{\text{eff},i}$ = effective diffusion coefficient of compound i ($\text{cm}^2\cdot\text{s}^{-1}$)
- $D_{i,l}^{\text{inf}}$ = infinite-dilution molecular diffusion coefficient of solute i in solvent l ($\text{cm}^2\cdot\text{s}^{-1}$)
- $D_{i,\text{mix}}$ = diffusion coefficient of compound i in a mixture ($\text{cm}^2\cdot\text{s}^{-1}$)
- E_a = reaction activation energy ($\text{kJ}\cdot\text{mol}^{-1}$)
- ΔG^0 = standard reaction Gibbs free energy ($\text{kJ}\cdot\text{mol}^{-1}$)
- $\Delta G_{f,i}^0$ = standard Gibbs free energy of formation of compound i ($\text{kJ}\cdot\text{mol}^{-1}$)
- ΔH^0 = standard reaction enthalpy ($\text{kJ}\cdot\text{mol}^{-1}$)
- $\Delta H_{f,i}^0$ = standard enthalpy of formation of compound i ($\text{kJ}\cdot\text{mol}^{-1}$)

$\Delta H_{W,S}$ = enthalpy of adsorption of water ($\text{kJ}\cdot\text{mol}^{-1}$)
 K = reaction equilibrium constant
 k_c = reaction kinetic constant ($\text{mol}\cdot\text{g}_{\text{cat}}^{-1}\cdot\text{min}^{-1}$)
 k_{c0} = Arrhenius pre-exponential factor for the reaction kinetic constant ($\text{mol}\cdot\text{g}_{\text{cat}}^{-1}\cdot\text{min}^{-1}$)
 $K_{S,W}$ = adsorption equilibrium constant of water
 $K_{S,W0}$ = van't Hoff pre-exponential factor for the adsorption equilibrium constant of water
 ΔM^0 = standard property change for a reaction
 N = total number of measurements during all kinetic experiments
 NE = number of kinetic experiments performed
 NM_j = number of measurements of conversion values taken in kinetic experiment j
 P = pressure (bar)
 Q_n = UNIFAC surface-area contribution parameter for group n
 r = radial position (cm)
 $r_{\text{Acet/Gly}}$ = initial molar ratio of reactants
 R = ideal gas constant ($\text{kJ}\cdot\text{mol}^{-1}\cdot\text{K}^{-1}$)
 R_n = UNIFAC volume contribution parameter for group n
 R_p = radius of a catalyst particle (μm)
 R = reaction rate based on the local intraparticle composition ($\text{mol}\cdot\text{g}_{\text{cat}}^{-1}\cdot\text{min}^{-1}$)
 ΔS^0 = reaction standard entropy change ($\text{kJ}\cdot\text{mol}^{-1}\cdot\text{K}^{-1}$)
 T = temperature (K)
 t = time (min)
 $V_{M,i}$ = liquid molar volume of compound i ($\text{cm}^3\cdot\text{mol}^{-1}$)
 wt_{cat} = catalyst loading (wt %)
 x_i = molar fraction of compound i
 X_{jk}^{exp} = k th value for the conversion measured in experiment j
 X_{jk}^{mod} = k th value for the conversion in experiment j predicted by the model

Greek Symbols

$\alpha_{m,n}$ = UNIFAC group interaction parameter
 γ_i = activity coefficient for compound i
 ε_b = catalyst particle porosity
 ε_p = bulk porosity
 θ = set of parameters to be estimated by the maximum likelihood method
 μ_i = viscosity of compound i (cP)
 μ_{mix} = mixture viscosity (cP)
 ν_i = stoichiometric coefficient of compound i
 ρ_i = density of compound i ($\text{g}\cdot\text{cm}^{-3}$)
 ρ_p = density of catalyst particles ($\text{g}\cdot\text{cm}^{-3}$)
 σ_{jk}^2 = variance of the k th measurement of conversion in experiment j
 τ_p = tortuosity of catalyst particles
 Φ = maximum likelihood objective function

Subscripts

Ac = acetaldehyde
 b = bulk
 cat = catalyst
 f = formation
 GEA = GEA
 Gly = glycerol
 i = compound i
 j = j th experiment
 k = k th measurement
 l = compound l
 m, n = UNIFAC group index
 mix = mixture

p = particle
 W = water

Superscripts

0 = property at standard state
 exp = experimentally measured variable
 inf = property at infinite dilution
 mod = model-predicted variable

REFERENCES

- (1) Behr, A.; Eilting, J.; Irawadi, K.; Leschinski, J.; Lindner, F. Improved utilisation of renewable resources: New important derivatives of glycerol. *Green Chem.* **2008**, *10* (1), 13.
- (2) Mota, C. J. A.; Silva, C. X. A. D.; Gonçalves, V. L. C. Gliceroquímica: novos produtos e processos a partir da glicerina de produção de biodiesel. *Quím. Nova* **2009**, *32*, 639.
- (3) Zhou, C. H.; Beltramini, J. N.; Fan, Y. X.; Lu, G. Q. Chemoselective catalytic conversion of glycerol as a biorenewable source to valuable commodity chemicals. *Chem. Soc. Rev.* **2008**, *37* (3), 527.
- (4) Climent, M. J.; Corma, A.; Velty, A. Synthesis of hyacinth, vanilla, and blossom orange fragrances: The benefit of using zeolites and delaminated zeolites as catalysts. *Appl. Catal. A: Gen.* **2004**, *263* (2), 155.
- (5) Kohlpaintner, C.; Schulte, M.; Falbe, J.; Lappe, P.; Weber, J. Aldehydes, Aliphatic and Aromatic. In *Ullmann's Encyclopedia of Industrial Chemistry*; Wiley-VCH: Weinheim, Germany, 2000.
- (6) Delfort, B.; Durand, I.; Jaecker-Voirol, A.; Lacomme, T.; Montagne, X.; Paille, F. Diesel Fuel Compounds Containing Glycerol Acetals. U.S. Patent 6,890,364, 2003.
- (7) Jaecker-Voirol, A.; Durand, I.; Hillion, G.; Delfort, B.; Montagne, X. Glycerin for new biodiesel formulation. *Oil Gas Sci. Technol.* **2008**, *63*, 395.
- (8) García, E.; Laca, M.; Pérez, E.; Garrido, A.; Peinado, J. New class of acetal derived from glycerin as a biodiesel fuel component. *Energy Fuels* **2008**, *22*, 4274.
- (9) Delgado Puche, J. M. Procedure to obtain biodiesel fuel with improved properties at low temperature. U.S. Patent 7,637,969, 2009.
- (10) Mushrush, G. W.; Beal, E. J.; Hardy, D. R.; Hughes, J. M.; Cummings, J. C. Jet fuel system icing inhibitors: Synthesis and characterization. *Ind. Eng. Chem. Res.* **1999**, *38*, 2497.
- (11) Mushrush, G. W.; Beal, E. J.; Hardy, D. R.; Stalick, W. M.; Basu, S.; Grosjean, D.; Cummings, J. Jet fuel system icing inhibitors: Synthesis and stability. *Prepr. Pap.-Am. Chem. Soc., Div. Fuel Chem.* **1998**, *43*, 60.
- (12) Mushrush, G. W.; Stalick, W. M.; Beal, E. J.; Basu, S. C.; Eric Slone, J.; Cummings, J. The synthesis of acetals and ketals of the reduced sugar mannose as fuel system icing inhibitors. *Pet. Sci. Technol.* **1997**, *15*, 237.
- (13) Hillion, G.; Delfort, B.; Durand, I. Method for Producing Biofuels, Transforming Triglycerides into at Least Two Biofuel Families: Fatty Acid Monoesters and Ethers and/or Soluble Glycerol Acetals. U.S. Patent Application 2007/0283619 A1, 2007.
- (14) Varfolomeev, S. D.; Nikiforov, G. A.; Volieva, V. B.; Makarov, G. G.; Trusov, L. I. Agent for Increasing the Octane Number of a Gasoline Automobile Fuel. WO Patent 2009/145674, 2009.
- (15) Da Silva Ferreira, A. C.; Barbe, J. C.; Bertrand, A. Heterocyclic acetals from glycerol and acetaldehyde in port wines: Evolution with aging. *J. Agric. Food. Chem.* **2002**, *50*, 2560.
- (16) Harnitzky, T.; Menschutkine, N. Ueber die Verbindungen des Glycerins mit den Aldehyden. *Justus Liebigs Ann. Chem.* **1865**, *136*, 4.
- (17) Shevchuk, A. S.; Podgornova, V. A.; Piskaikina, E. G. Features of synthesis of 4-hydroxymethyl-1,3-dioxolanes from glycerol and aldehydes. *Russ. J. Appl. Chem.* **1999**, *72*, 853–856.
- (18) Nef, J. U. Dissociationsvorgänge in der Glycol-Glycerinreihe. *Justus Liebigs Ann. Chem.* **1904**, *335*, 191.
- (19) Hill, H. S.; Hill, A. C.; Hibbert, H. Studies on the Reactinos Relating to Carbohydrates and Polysaccharides. XVI. Separation and

Identification of the Isomeric Ethylidene Glycerols. *J. Am. Chem. Soc.* **1928**, *50*, 2242.

(20) Martin Maglio, M.; Burger, C. A. Condensation reactions: A laboratory preparation of ethylidene glycerol. *J. Chem. Educ.* **1946**, *23*, 174.

(21) Miller, D. J.; Peereboom, L.; Kolah, A. K.; Asthana, N. S.; Lira, C. T. Process for production of a composition useful as a fuel. U.S. Patent 2006/0199970 A1, 2008.

(22) Hong, X.; Kolah, A. K.; Lira, C. T.; Miller, D. J. An improved approach for cyclic acetals from glycerol. Presented at the *AIChE Annual Meeting*, Nashville, TN, Nov 8–13, 2009.

(23) Hong, X.; McGiveron, O.; Lira, C. T.; Orjuela, A.; Peereboom, L.; Miller, D. J. A Reactive Distillation Process To Produce 5-Hydroxy-2-methyl-1,3-dioxane from Mixed Glycerol Acetal Isomers. *Org. Process Res. Dev.* **2011**, *16*, 1141.

(24) Silva, V. M. T. M.; Rodrigues, A. E. Novel process for diethylacetal synthesis. *AIChE J.* **2005**, *51*, 2752.

(25) Rodrigues, A. E.; Silva, V. M. T. M. Industrial Process for Acetals Production in a Simulated Moving Bed Reactor. PT Patent 103123; WO Patent 2005/113476A1; U.S. Patent 2008/0287714; EP Patent 1748974, 2004.

(26) Pereira, C. S. M.; Gomes, P. S.; Gandi, G. K.; Silva, V. M. T. M.; Rodrigues, A. E. Multifunctional Reactor for the Synthesis of Dimethylacetal. *Ind. Eng. Chem. Res.* **2007**, *47*, 3515.

(27) Graça, N. S.; Pais, L. S.; Silva, V. M. T. M.; Rodrigues, A. E. Analysis of the synthesis of 1,1-dibutoxyethane in a simulated moving-bed adsorptive reactor. *Chem. Eng. Process.: Process Intensif.* **2011**, *50*, 1214.

(28) Constable, D. J. C.; Curzons, A. D.; Cunningham, V. L. Metrics to 'green' chemistry—Which are the best? *Green Chem.* **2002**, *4*, 521.

(29) Miller, D. J.; Hong, X.; Lira, C. T.; McGiveron, O. Methods for Making 1,3-Dihydroxyacetone (DHA) from Glycerol. U.S. Patent 2012/0014889 A1, 2012.

(30) Ruiz, V. R.; Vely, A.; Santos, L. L.; Leyva-Pérez, A.; Sabater, M. J.; Iborra, S.; Corma, A. Gold catalysts and solid catalysts for biomass transformations: Valorization of glycerol and glycerol-water mixtures through formation of cyclic acetals. *J. Catal.* **2010**, *271*, 351.

(31) da Silva, C. X. A.; Gonçalves, V. L. C.; Mota, C. J. A. Water-tolerant zeolite catalyst for the acetalisation of glycerol. *Green Chem.* **2009**, *11*, 38.

(32) Silva, P. H. R.; Gonçalves, V. L. C.; Mota, C. J. A. Glycerol acetals as anti-freezing additives for biodiesel. *Bioresour. Technol.* **2010**, *101*, 6225.

(33) Deutsch, J.; Martin, A.; Lieske, H. Investigations on heterogeneously catalysed condensations of glycerol to cyclic acetals. *J. Catal.* **2007**, *245*, 428.

(34) Ballini, R.; Bosica, G.; Frullanti, B.; Maggi, R.; Sartori, G.; Schroer, F. 1,3-Dioxolanes from carbonyl compounds over zeolite HSZ-360 as a reusable, heterogeneous catalyst. *Tetrahedron Lett.* **1998**, *39*, 1615.

(35) Umbarkar, S. B.; Kotbagi, T. V.; Biradar, A. V.; Pasricha, R.; Chanale, J.; Dongare, M. K.; Mamede, A. S.; Lancelot, C.; Payen, E. Acetalization of glycerol using mesoporous MoO₃/SiO₂ solid acid catalyst. *J. Mol. Catal. A: Chem.* **2009**, *310*, 150.

(36) Iwamoto, M.; Tanaka, Y.; Sawamura, N.; Namba, S. Remarkable Effect of Pore Size on the Catalytic Activity of Mesoporous Silica for the Acetalization of Cyclohexanone with Methanol. *J. Am. Chem. Soc.* **2003**, *125*, 13032.

(37) Tanaka, Y.; Sawamura, N.; Iwamoto, M. Highly effective acetalization of aldehydes and ketones with methanol on siliceous mesoporous material. *Tetrahedron Lett.* **1998**, *39*, 9457.

(38) Agirre, I.; García, I.; Requies, J.; Barrio, V. L.; Güemez, M. B.; Cambra, J. F.; Arias, P. L. Glycerol acetals, kinetic study of the reaction between glycerol and formaldehyde. *Biomass Bioenergy* **2011**, *35*, 3636.

(39) *DIPPR 801 Database*; AIChE: New York, 2012.

(40) Quinta-Ferreira, R. M.; Almeida-Costa, C. A.; Rodrigues, A. E. Heterogeneous models of tubular reactors packed with ion-exchange resins: Simulation of the MTBE synthesis. *Ind. Eng. Chem. Res.* **1996**, *35*, 3827.

(41) Ihm, S. K.; Ahn, J. H.; Jo, Y. D. Interaction of reaction and mass transfer in ion-exchange resin catalysts. *Ind. Eng. Chem. Res.* **1996**, *35*, 2946.

(42) Dogu, T.; Aydin, E.; Boz, N.; Murtezaoglu, K.; Dogu, G. Diffusion resistances and contribution of surface diffusion in TAME and TAE production using Amberlyst-15. *Int. J. Chem. React. Eng.* **2003**, *1*, A6.

(43) Sundmacher, K.; Zhang, R. S.; Hoffmann, U. Mass-transfer effects on kinetics of nonideal liquid-phase ethyl *tert*-butyl ether formation. *Chem. Eng. Technol.* **1995**, *18*, 269.

(44) Silva, V. M. T. M.; Rodrigues, A. E. Kinetic studies in a batch reactor using ion exchange resin catalysts for oxygenates production: Role of mass transfer mechanisms. *Chem. Eng. Sci.* **2006**, *61*, 316.

(45) Yaws, C. L. *Yaws' Handbook of Physical Properties for Hydrocarbons and Chemicals*; Knovel: New York, 2008.

(46) Gandi, G. K.; Silva, V. M. T. M.; Rodrigues, A. E. Process development for dimethylacetal synthesis: Thermodynamics and reaction kinetics. *Ind. Eng. Chem. Res.* **2005**, *44*, 7287.

(47) Silva, V. M. T. M.; Rodrigues, A. E. Synthesis of diethylacetal: Thermodynamic and kinetic studies. *Chem. Eng. Sci.* **2001**, *56*, 1255.

(48) Graça, N. S.; Pais, L. S.; Silva, V. M. T. M.; Rodrigues, A. E. Oxygenated biofuels from butanol for diesel blends: Synthesis of the acetal 1,1-dibutoxyethane catalyzed by amberlyst-15 ion-exchange resin. *Ind. Eng. Chem. Res.* **2010**, *49*, 6763.

(49) Xu, Z. P.; Chuang, K. T. Effect of internal diffusion on heterogeneous catalytic esterification of acetic acid. *Chem. Eng. Sci.* **1997**, *52*, 3011.

(50) Levenspiel, O. *Chemical Reaction Engineering*, 3rd ed.; John Wiley & Sons: New York, 1998.

(51) Pöpken, T.; Götze, L.; Gmehling, J. Reaction kinetics and chemical equilibrium of homogeneously and heterogeneously catalyzed acetic acid esterification with methanol and methyl acetate hydrolysis. *Ind. Eng. Chem. Res.* **2000**, *39*, 2601.